Available online at www.sciencedirect.com
SCIENCE DIRECT®
Journal of Solid State Chemistry 178 (2005) 3715–3721
JOURNAL OF SOLID STATE CHEMISTRY
www.elsevier.com/locate/jssc

Synthesis and structure investigation of the $Pb_3V(PO_4)_3$ eulytite

Roman V. Shpanchenko[a,*], Rodion V. Panin[a], Joke Hadermann[b], Catherine Bougerol[c], Eiji Takayama-Muromachi[d], Evgeny V. Antipov[a]

[a]*Department of Chemistry, Moscow State University, 119992 Moscow, Russia*
[b]*EMAT University of Antwerp (RUCA), Groenenborgerlaan 171, 2020 Antwerp, Belgium*
[c]*Equipe NPSC DRFMC/SP2 M CEA Grenoble, 17 rue des Martyrs, 38054 Grenoble cedex France*
[d]*NIMS, 1-1 Namiki, Tsukuba, Ibaraki 305-0044, Japan*

Received 2 August 2005; received in revised form 16 September 2005; accepted 16 September 2005
Available online 2 November 2005

Abstract

Lead vanadium phosphate $Pb_3V(PO_4)_3$ was synthesized by solid state reaction and characterized by X-ray single crystal and powder diffraction, electron microscopy, and magnetic susceptibility measurements. The crystal structure model of $Pb_3V(PO_4)_3$ was refined using X-ray single crystal data ($a = 10.127(1)$ Å, S.G. $I\bar{4}3d$, $Z = 4$). The compound has an eulytite-like structure and its average structure model may be presented as a three-dimensional network formed by strongly distorted mixed (Pb/V^{III}) metal-oxygen octahedra connected by edge sharing and forming corrugated chains. The octahedra are additionally linked by tetrahedral phosphate groups via corner sharing. Lead and vanadium atoms randomly occupy two close positions in the octahedra. The electron microscopy study revealed the presence of a rhombohedral superstructure with $a_{sup} = a_{sub} \times \sqrt{2}$ and $c_{sup} = c_{sub} \times \sqrt{75}/2$ indicating ordering in the structure. The same type of superstructure was found by us for two another lead-containing eulytite $Pb_3Fe(PO_4)_3$ where Fe^{+3} has an ionic radius close to that of V^{+3}. Magnetic susceptibility measurements revealed Curie–Weiss behavior for the $Pb_3V(PO_4)_3$ compound.

Keywords: Lead vanadium phosphate; Eulytite; Superstructure; Magnetic properties

1. Introduction

Over the last ten years the luminescent properties of eulytite-like compounds are widely investigated due to their possible application, for instance, in mercury-free lamps, plasma display panels or powder laser materials [1–5]. Among the complex phosphates of di- and trivalent cations with the $M_3^{II}M^{III}(PO_4)_4$ composition eulytite-like compounds form a quite numerous family. M^{II} may be an alkali-earth element [6–8], Eu^{II} or Pb [9] and M a rare-earth, Bi [6–10] or transition metal [9].

The eulytite structure $M_3^{II}M^{III}(PO_4)_4$ (S.G. $I\bar{4}3d$) contains strongly distorted mixed (M^{II}/M^{III}) metal-oxygen octahedra connected by edge sharing and forming corrugated chains. The octahedra are additionally linked by tetrahedral phosphate groups via corner sharing (Fig. 1). Structural investigations of different eulytites were carried out mainly by powder X-ray and neutron diffraction techniques. Only three papers reported single crystal structure determination, namely, for $Ba_3Bi(PO_4)_3$ [8], $Pb_4(PO_4)_2SO_4$ [11] and $Na_3Bi_5(PO_4)_6$ [10]. The two latter compounds also have an eulytite-like structure but different oxidation sates of the M-cations ($Pb^{+2} + Pb^{+4}$ and $Na^{+1} + Bi^{+3}$) result in other cation ratios. The main structural feature of almost all eulytite-like compounds is a presence of different types of disorder in the cation or anion (or both) frameworks. An electron diffraction study was carried out only for $Ca_3Bi(PO_4)_3$ [7] and no deviation from the cubic $I\bar{4}3d$ space group was found.

Most of the investigated eulytites contain in their structures cations comparable by ionic radii like an alkali-earth metal and a rare-earth (or Bi) metal, etc. At the same time the existence of the $Pb_3M(PO_4)_3$ was reported for M = Sc–Fe i.e. for cations with an ionic radius almost twice smaller than that of Pb^{+2} [9,12]. Nevertheless, no other information except lattice parameters for these compounds was published. In the frame of

*Corresponding author. Fax: +7 095 939 47 88
E-mail address: shpanchenko@icr.chem.msu.ru (R.V. Shpanchenko).

0022-4596/$ - see front matter © 2005 Elsevier Inc. All rights reserved.
doi:10.1016/j.jssc.2005.09.045

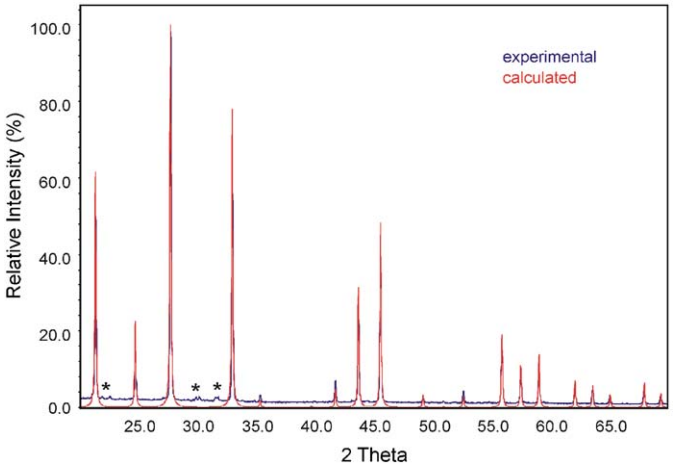

Fig. 1. Experimantal and calculated XPD patterns for $Pb_3V(PO_4)_3$. Admixture peaks of $Pb_3V_2(PO_4)_4$ are marked by stars.

our research on the Pb–V^{+3}–P–O system we present the preparation of the $Pb_3V(PO_4)_3$ eulytite, its crystal structure determination, electron microscopy study and magnetic properties measurements.

2. Experimental

A yellow-brown powder sample of $Pb_3V(PO_4)_3$ was prepared in two steps and contained a small amount ($I_{max} \approx 3\%$) of another new phosphate $Pb_3V_2(PO_4)_4$ [13] isostructural with $Pb_3Cr_2(PO_4)_4$ [14]. At the beginning a stoichiometric mixture of $Pb_2P_2O_7$ and V_2O_3 was stirred under acetone, pressed in pellets and annealed at 900 °C for 36 h in an evacuated quartz ampoule. Then the temperature was raised up to 990 °C followed by quenching the ampoule into water. Small crystals used for X-ray analysis were formed on the surface of the quenched pellet. Quenching from 900 °C or slow cooling of the reaction mixture always resulted in a formation of polyphasic mixtures. From the other side an increase of the annealing temperature led to an acceleration of red-ox processes and metallic lead drops, VO_2, and unknown impurities were present in the samples. $Pb_2P_2O_7$ was synthesized by heating the equimolar mixture of PbO and $(NH_4)H_2PO_4$ at 700°C in air for 3 days with intermediate regrinding. V_2O_3 was prepared by reducing V_2O_5 at 540 and 800°C in hydrogen flow. $Pb_3Cr(PO_4)_3$ and $Pb_3Fe(PO_4)_3$ were synthesized from $Pb_2P_2O_7$ and the corresponding oxides according to [15,16], respectively.

X-ray powder diffraction (XRPD) data were collected on a STOE STADI/P (transmission mode, Cu$K\alpha$1-radiation, Ge-monochromator, linear-PSD) and RINT2000 (Cu$K\alpha$-radiation, scintillation counter) powder diffractometers. Single crystal data collection was performed on a CAD-4 diffractometer. The structure model refinement for $Pb_3V(PO_4)_3$ was carried out with the GSAS [17] and CSD [18] programs with powder and single crystal data, respectively. Transmission electron microscopy (EM) was performed with Philips CM20 (electron diffraction) and JEOL 4000EX (high resolution electron microscopy (HREM) images) microscopes. HREM image simulation was done using the MacTempas software. The magnetic susceptibility measurements were carried out with Quantum Design MPMS SQUID magnetometer 0.01, 0.1 and 1 T magnetic fields between 2 and 400 K.

3. Results

3.1. Structure model refinement of $Pb_3V(PO_4)_3$

The XRPD pattern of $Pb_3V(PO_4)_3$ was indexed in a cubic lattice with the parameter $a = 10.1229(4)$Å. Only reflections with $h + k + l = 2n$ were present indicating the I-centered unit cell. Almost all eulytite phosphates crystallize in the $I\bar{4}3d$ space group. Further analysis of our X-ray pattern also revealed as additional reflection conditions hhl: $2h + l = 4n$, $0kl$: $k + l = 2n$ and $h00$: $h = 4n$.

The single crystal data of $Pb_3V(PO_4)_3$ were indexed with almost the same cell parameter (10.127(1) Å). The data collection was done for primitive unit cell and 279 collected reflections confirmed the set of the reflection conditions resulting in the $I\bar{4}3d$ space group. However, only 58 independent reflections were used for structure refinement after $I > 3\sigma(I)$ restriction. Atomic coordinates for the $Pb_3V(PO_4)_3$ starting model were taken from the $Ca_3Bi(PO_4)_3$ crystal structure [7]. The refinement was carried out in block mode where successively only one atom per iteration was refined. The Pb:V ratio was fixed as 3:1 and was not refined. The atomic displacement parameters were refined only for the metals whereas those for phosphorus and oxygen atoms were refined simultaneously to reduce the number of refined parameters. During the refinement the 16c position occupied initially by both Pb (75%) and V (25%) atoms was found to be split into two positions with the close x-coordinates. Therefore, the metal atoms were separated into different positions with a separation of 0.464(15) Å. The best refinement result was found for the first position filled by 75% lead whereas the second position was found to be filled by 25% vanadium. A placement of the phosphorus atom in the ideal $\frac{3}{8}$;0;$\frac{1}{4}$ (12a) position with 100% occupancy (as it was found in the $Ca_3Bi(PO_4)_3$ structure resulted in an enormously high value for the displacement parameter for this atom (up to 6 $Å^2$) and the R-factor becomes 3% higher. Therefore, the 12a phosphorus atom position was split into a 48e position with statistical occupancy of 25%. The refinement of the position and occupancy for the oxygen atoms also revealed a strong disorder in the anion sublattice. Three different positions were found and all of them are only partially occupied. The total amount of oxygen atoms found from the refinement is 43.4($\pm$1.5) atoms per unit cell which is close to the theoretical amount of 48. Actually, there were a few weak maxima on the difference Fourier map which may be attributed to partially occupied oxygen positions. For instance, a refinement of these peaks as oxygen atoms resulted in occupancies about 0.05 that corresponds to

nearly 2.5 atoms per 48-fold position. Since all oxygen atoms belong to phosphate groups the number of oxygen atoms per unit cell must be 48. However, due to strong structural disorder only three positions may be reliably determined from our experiment. We failed to find better solution in the low symmetry subgroups: $I2_13$, $P2_13$ or even $P2_12_12_1$ space groups aiming to find more ordered model. A use of the found structural model for Rietveld refinement resulted in a good agreement between the calculated and observed X-ray powder patterns (Fig. 1). The experimental and crystallographic parameters for $Pb_3V(PO_4)_3$ are listed in Table 1. The atomic positions, displacement parameters and main interatomic distances in the $Pb_3V(PO_4)_3$ structure are given in Tables 2 and 3, respectively.

The crystal structure model of $Pb_3V(PO_4)_3$ may be described as a three-dimensional framework of edge and corner-shared metal-oxygen octahedra MO_6 (where $M = (Pb + V)$ in ratio Pb:V = 3:1) and PO_4-tetrahedra which is schematically represented in Fig. 2. For an easier presentation of the structural motif the symmetrically close but partially occupied atomic positions are shown as one average. The octahedra in the structure are strongly distorted as it usually happens in the eulytite structure and their connections is shown in Fig. 3. However, it is

Table 1
Experimental and crystallographic parameters for $Pb_3V(PO_4)_3$

Chemical formula	$Pb_3V(PO_4)_3$
Molecular weight	957.45
Crystal system	Cubic
Space group (No)	*I*-43*d* [220]
Cell constants (Å)	10.127(1)
Volume (Å^3)	1038.6(3)
Z	4
D_{calc}, (g cm^{-3})	6.136
Radiation and wavelength (Å)	Mo*K*α, 0.71073
Max θ (deg)	35.6
μ (cm^{-1})	492.24
Crystal size (mm)	$0.1 \times 0.07 \times 0.05$
Colour	Yellow-brown
Diffractometer	CAD4
Absorption correction	Ψ-scan
No. of measured refl.	279
No. of independent refl. $I > 3\sigma(I)$	58
Range of *h*, *k*, *l*	$0 \rightarrow h \rightarrow 16$ $0 \rightarrow k \rightarrow 16$ $0 \rightarrow l \rightarrow 16$
Reliability factor	$R_F = 0.020$
Goodness of fit	1.230
Package for structure refinement	WinCSD
Refinement on	*F*
No. of refined parameters	23
Weighting scheme	Unit

Table 3
Selected interatomic distances (Å) in the $Pb_3V(PO_4)_3$ structure

V–Pb	0.464(15)
V–O(2)	$3 \times 2.01(3)$
O(3)	$3 \times 2.33(4)$
Pb–O(3)	$3 \times 2.07(4)$
O(2)	$3 \times 2.31(3)$
O(2)	$3 \times 2.64(3)$
O(1)	$3 \times 2.72(4)$
P–O(1)	1.28(4), 1.42(4)
O(2)	1.43(4), 1.58(4), 1.88(4)
O(3)	1.18(4), 1.64(4), 1.65(4)

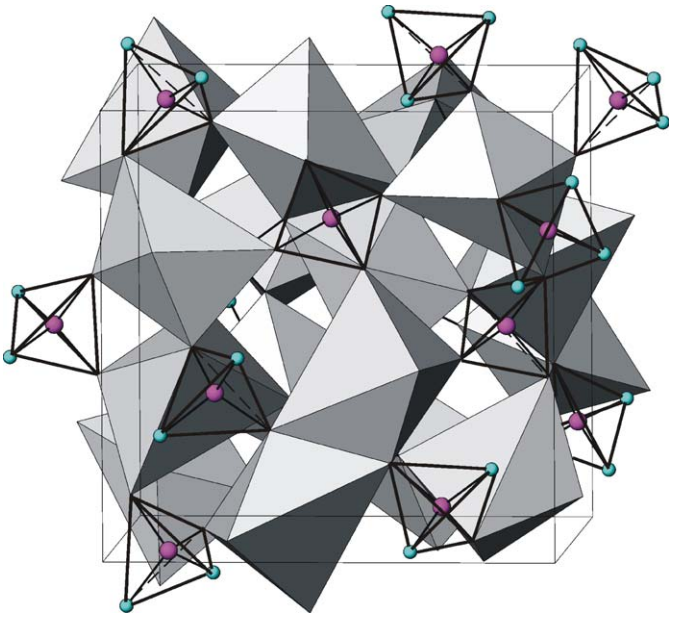

Fig. 2. Schematic representation of the $Pb_3V(PO_4)_3$ crystal structure. Pb/V and P atoms are situated in octahedra and tetrahedra, respectively.

Table 2
Atomic positions and displacement parameters in $Pb_3V(PO_4)_3$

Atom	Position	*x*/*a*	*y*/*b*	*z*/*c*	B_{iso}	*G*
V	16*c*	0.0974(14)	*x*	*x*	0.4(2)	0.25
Pb	16*c*	0.0712(1)	*x*	*x*	1.93(6)	0.75
P	48*e*	0.355(2)	−0.019(3)	0.220(2)	2.0(2)	0.25
O(1)	24*d*	3/4	0.009(5)	0	2.0*	0.39(3)
O(2)	48*e*	0.286(3)	0.058(3)	0.146(3)	2.0*	0.41(3)
O(3)	48*e*	0.367(4)	0.029(4)	0.119(4)	2.0*	0.30(3)

*Fixed parameter

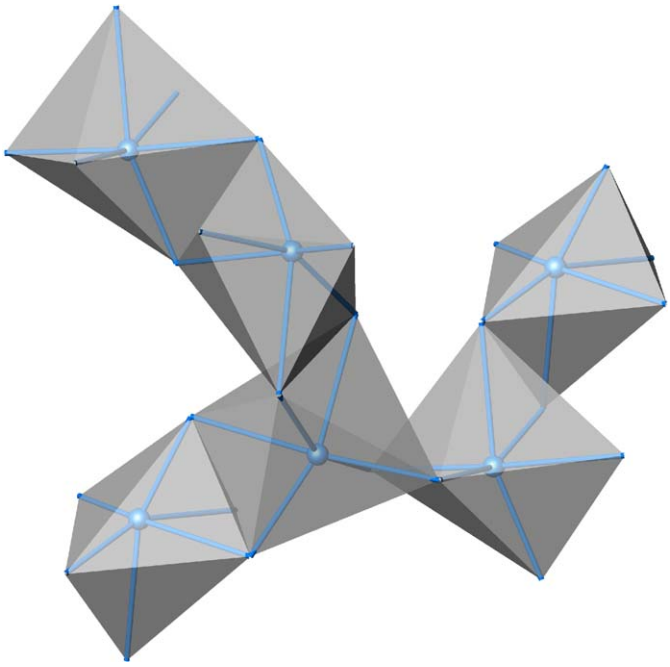

Fig. 3. Connection of the MO_6 octahedra in ideal eulytite structure.

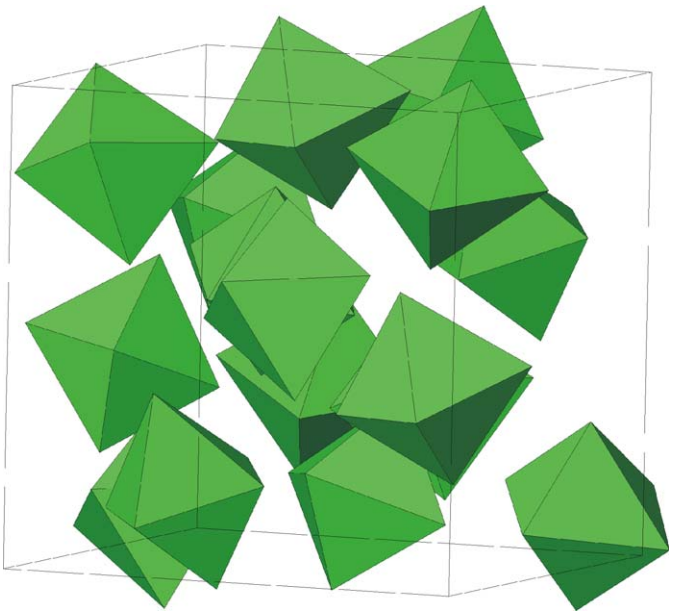

Fig. 4. VO_6 ocnahedra in the $Pb_3V(PO_4)_3$ structure.

interesting to consider the closest coordination arrangement for two separate metal positions. So, vanadium atom has ten oxygen neighbors statistically occupied. But if one chooses only O(2) and O(3) atoms separated from V by 2.01(3) and 2.33(4) Å, respectively, then the coordination polyhedron for the vanadium atom is a slightly distorted octahedron (Fig. 4). It is noteworthy that such VO_6 octahedra do not share their vertices or edges. The coordination arrangement for Pb-position cannot be easily deduced since the lead atoms may have high coordination numbers in comparison with V^{+3} having only an octahedral environment. Nevertheless, the average Pb–O distances are noticeably longer than the V–O ones (see Table 3).

P–O distances are in the range of 1.04(6)–1.88(4)Å. Taking into account the number of distances and occupancies there seems to be a random orientation of the phosphate group inside this structure model. Among a big variety of the P–O distances one may separate eight ones in the range of 1.18–1.88 Å which may be chosen to form strongly distorted tetrahedra for every phosphorus atom in this split position. Since the phosphate group is a quite rigid unit in the inorganic structures one may suggest that its distortion (as well as random orientation) found in the $Pb_3V(PO_4)_3$ structure is a consequence of the existence of ordering in the real structure.

Thus, the unusually high disorder degree in the $Pb_3V(PO_4)_3$ structure in comparison with already known eulytite-like structures may indicate a presence of cation and/or anion ordering which is not visible in the X-ray patterns for some reasons. The two different positions for the Pb and V atoms and the high values of the displacement parameters indirectly confirm this suggestion. Therefore, we performed an electron microscopy study of two cubic eulytites $Pb_3M(PO_4)_3$ with $M = V$ and Fe. The Fe^{+3} cation was chosen for comparison since it has an ionic radius of 0.785 Å which is close to the vanadium radius (0.78 Å).

3.2. EM study of $Pb_3M(PO_4)_3$ eulytites with $M = V$ and Fe

The electron microscopy study for $Ca_3Bi(PO_4)_3$ [7] did not reveal any superstructure. However, when studying the samples of $Pb_3M(PO_4)_3$ with $M = V$, Fe a clear superstructure was observed on the electron diffraction patterns. Fig. 5 shows the electron diffraction patterns of the main zones of $Pb_3V(PO_4)_3$. On these patterns a clear superstructure is present compared to the cell determined from X-ray diffraction. The boldest reflections belong to the subcell and can be indexed using the cubic cell with the cell parameters as determined from the X-ray diffraction data $a = 10.127$ Å. The finer reflections belong to the superstructure and can be indexed using a rhombohedral supercell with the approximate cell parameters $a = b = 14.3$ Å and $c = 43.9$ Å, $\alpha = \beta = 90^\circ$, $\gamma = 120^\circ$. The $[\bar{1}2\bar{1}0]^*_s$ pattern is made up of a combination of three twins, a scheme representing a single twin is put at the right side of this pattern. The correspondence between the zones of these electron diffraction patterns in the rhombohedral cell, and the cubic cell are $[\bar{1}2\bar{1}0]^*_s = [101]_c{}^*$, $[10\bar{1}1]^*_s = [131]_c{}^*$ and $[0001]_s{}^* = [111]_c{}^*$, where the subscript c refers to the cubic subcell and s to the rhombohedral supercell. The transformation matrix between the cubic subcell and the rhombohedral supercell is

$$\begin{bmatrix} -1 & 1 & 0 \\ 1 & 0 & -1 \\ 5/2 & 5/2 & 5/2 \end{bmatrix}.$$

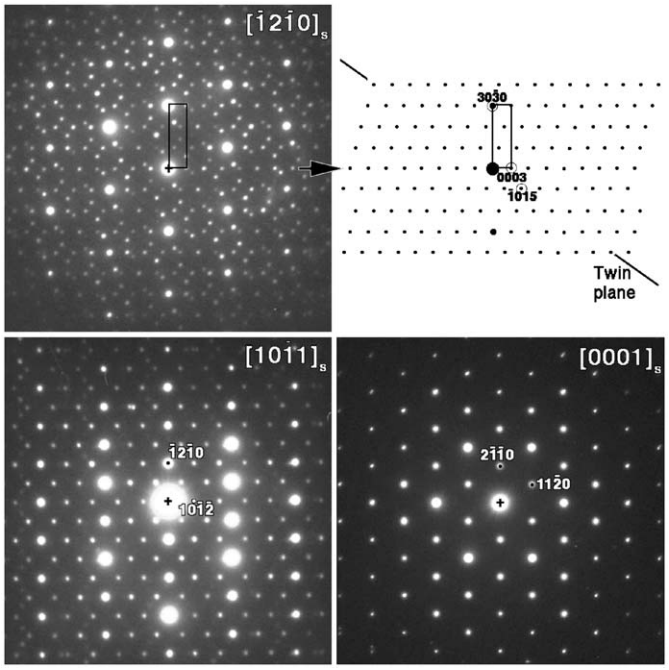

Fig. 5. Electron diffraction patterns of the main zones of $Pb_3V(PO_4)_3$. The indexation is made in the trigonal supercell. The scheme at the left of the $[\bar{1}2\bar{1}0]^*_s$ pattern shows one of the two twins present in the $[\bar{1}2\bar{1}0]^*_s$ pattern and the indexation of this twin.

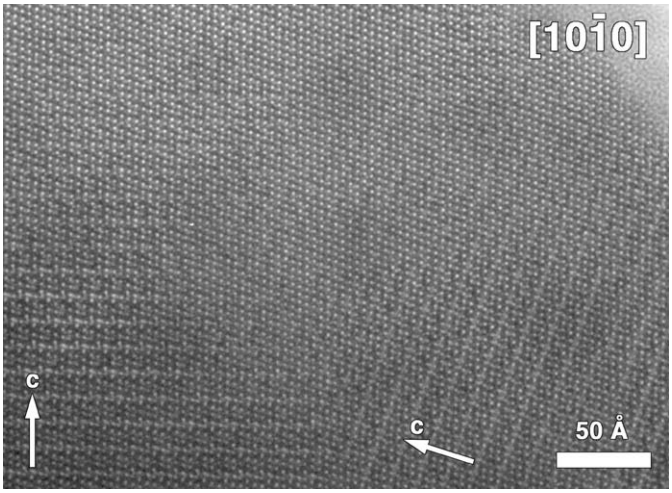

Fig. 6. High resolution electron microscopy image of $Pb_3V(PO_4)_3$ showing two twin variants. The white dots correspond to the projection of the columns of lighter atoms in between the cations Pb and V, which are themselves projected as the dark areas in between the bright dots.

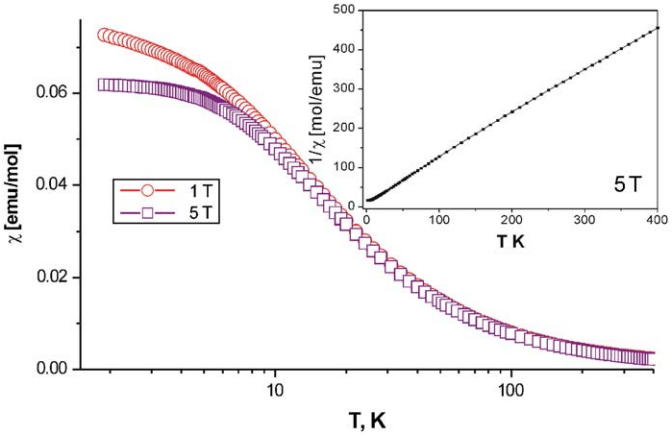

Fig. 7. $\chi(T)$ and $1/\chi(T)$ (insert) dependences for $Pb_3V(PO_4)_3$.

The reflection conditions which can be derived from the different electron diffraction patterns are $hkil: -h+k+l=3n$, $hh;-0l: h+l=3n$ and $0\,0\,0\,l: l=3n$, which are in agreement with the extinction symbol R- -, and lead to a limitation of the possible space groups to $R3$, $R\bar{3}$, $R32$, $R3m$ and $R\bar{3}m$.

The material $Pb_3Fe(PO_4)_3$ was also studied using electron diffraction. It shows the same superstructure as $Pb_3V(PO_4)_3$ and could be indexed using the same extinction symbol R- - and the approximate cell parameters $a=b=14.4$ Å and $c=44$ Å.

On the high resolution image of the $[\bar{1}2\bar{1}0]^*_s$ zone in Fig. 6, the white dots represent the columns of lighter atoms in between the cations. The dark areas represent the cations (Pb, V). The high resolution electron microscopy images show that the crystals consist of domains with mirror-twins. The twins have a common sublattice, but the superlattice is mirrored over the reciprocal plane including the zone-axis and the reflection $(\bar{1}015)$, this reflection corresponds to the (101) reflection in the subcell indexation. The size of these domains is on average smaller than 30 nm in diameter, which can explain why the superstructure reflections are not visible on the XRD patterns and only the subcell is detected there.

3.3. Magnetic properties of $Pb_3V(PO_4)_3$

The $1/\chi(T)$ dependence for $Pb_3V(PO_4)_3$ is presented in Fig. 7. It follows the Curie–Weiss (CW) law with $\theta=-31$ K without any noticeable deviations for almost the whole measured temperature range. The effective magnetic moment calculated in the temperature range of 200–400 K is 2.75 μ_B. It is close to the expected value for the isolated V^{+3} ion of 2.83 μ_B calculated according to $\mu_{eff}=g\sqrt{s(s+1)n}$ for $S=1$ (for d^2 ion). At 10 K a deviation from the CW dependence occurs, probably due to superexchange between VO_6 octahedra connected via phosphate groups. $Pb_3V_2(PO_4)_3$ which is present as an admixture (about 3 wt%) exhibits also paramagnetic behavior and scarcely influences the view of the susceptibility curve. The paramagnetic behavior can be easily explained by the structural features of the $Pb_3V(PO_4)_3$ phosphate. So, the cation ordering supposed from the XRD data and proven by the EM study should result in the isolated placement of vanadium atoms like it was observed in the $Pb_3V_2(PO_4)_3$ [13] and $Pb_{1.5}V_2(PO_4)_3$ [19] structures. Therefore, at high temperatures the V^{+3} cations behave like isolated ($S=1$)

ions whereas interactions via indirect ways become possible at low temperature. One should note that an increase of the applied field results to increase of the deviation from the CW behavior.

4. Discussion

$Pb_3V(PO_4)_3$ investigated in the frame of this work is the third lead vanadium phosphate after $PbV_2(P_2O_7)_2$ [20] and $Pb_{1.5}V_2(PO_4)_3$ [19] containing only V^{+3} in their structures. The synthesis of the compounds containing V^{+3} and Pb^{+2} may be difficult due to a possible red-ox reaction between these cations. Indeed, we observed drops of metallic lead in the sample after increasing the annealing temperature above 900 °C.

Barbier [11,21] analyzing the synthetic conditions for $Sr_4(PO_4)_2(CrO_4)$ [22] and Pb-containing eulytites $Pb_4(PO_4)_2(CrO_4)$ and $Pb_4(PO_4)_2(SO_4)$ concluded that the presence of a lone pair of the lead atom stabilizes the eulytite structure. Very likely, $Pb_3V(PO_4)_3$ is not an exception from this rule. It was obtained at 900 °C whereas we failed to synthesize "$Sr_3V(PO_4)_3$" eulytite and instead another compound, namely $Sr_9V(PO_4)_7$, with whitlockite-like structure is formed [23]. It is known that many eulytites can be obtained only by quenching from high temperatures. In the case of $Pb_3V(PO_4)_3$ the situation is even more complicated since the temperature range for its synthesis was found to be very narrow and restricted by kinetic reasons at the low temperature side and by red-ox processes at the high temperature side.

Eulytite-like structures often exhibit different types of disorder. The first classification of the disorder in the eulytite-like materials was presented by Arbib et al. [8]. They suggested four categories:

- completely ordered structures (like $Bi_4(XO_4)_3$ (X = Si, Ge) [24,25]);
- unique metal position and manifold oxygen sites (for instance, $Sr_3La(PO_4)_3$ [6], $Ca_3Bi(PO_4)_3$ [7] or $Pb_4(PO_4)_2(SO_4)$ [11]);
- cation and anion multisite structures with the only representative $Ba_3Bi(PO_4)_3$ [8];
- structures with one anion and two cation positions like $Na_3Bi_5(PO_4)_3$ [10].

Obviously, $Pb_3V(PO_4)_3$ should belong to the third clause. However, we suggest to separate the $Pb_3M(PO_4)_3$ (M = V, Fe) phosphates into special category. The main reason for that is a presence of the well-pronounced superstructure which unambiguously indicates the complicated type of the ordering absent in other investigated eulitytes. This superstructure is visible only on TEM images whereas no superstructure reflections were observed either on the X-ray powder or in the single crystal data. The ordered structure observed by TEM forms small twinned domains as shown by the HREM images. These areas are too small to produce a well pronounced superstructure in the XRD pattern where only subcell reflections are seen. One should remind that electron microscopy study performed with other eulytites did not reveal any deviation from the cubic symmetry. In the case of $Pb_3V(PO_4)_3$ even low quality single crystal data allowed to conclude about ordering between Pb^{+2} and V^{+3} when the first coordination environment of vanadium atom was analyzed.

The existence of the ordering in the $Pb_3M(PO_4)_3$ (M = V, Fe and very likely Cr) structures is rather presumptive. Such conclusion may be done due to the big difference between the ionic radii of Pb^{+2} (1.32 Å) and V^{+3} (0.78 Å) ($r_{Pb} : r_V = 1.69$) that is much bigger than that for other known eulytites (for instance, for $Sr_3Bi(PO_4)_3$ $r_{Sr}:r_{Bi} = 1.12$ and for $Ba_3Y(PO_4)_3$ $r_{Ba}:r_{Yb} = 1.50$). This may be a reason also why $Pb_3V(PO_4)_3$ exists only at high temperature and can be obtained by quenching, and completely decomposes being annealed at 300 °C during a few days. On the other hand, the twinning type observed in the ED patterns often takes place when structural transitions occur. Therefore, we cannot exclude that a disordered cubic eulytite phase exists at high temperature close to decomposition temperature.

A reversible structural transition from high temperature cubic eulytite to low temperature rhombohedral $Pb_3(PO_4)_2$-like cell was found earlier for the $Pb_4(PO_4)_2(CrO_4)$ [21] and $Sr_4(PO_4)_2(CrO_4)$ [22] compounds. This transition is accompanied by the appearance of a superstructure on the powder diffractograms that allowed to refine the crystal structure for the low-temperature phase. An additional superstructure of $a_{rhomb} \times 2$, $c_{rhomb} \times 2$ (somewhat similar to ours) was observed by electron diffraction for the Pb-containing compound. However, this weak superstructure was invisible on the XRD patterns. In our case we did not observe superstructural reflections on the XRD patterns for any $Pb_3M(PO_4)_3$ (M = V, Cr, Fe) compounds therefore no structural computation could be carried out. The real structure of $Pb_3M(PO_4)_3$ (M = V, Cr, Fe) may also be a derivative from the rhombohedral $Pb_3(PO_4)_2$ [26]. However, it is reasonable to suggest that the $Pb_3M(PO_4)_3$ structure will be different from that of rhombohedral $Pb_4(PO_4)_2(CrO_4)$. The main argument for this conclusion is the existence of isolated MO_6 octahedra in the ordered structure which are not present in the phosphate–chromate structure. Therefore, the whitlockite-like structure (which is closely related to the rhombohedral orthophosphate structure) is the most probable variant for the realization of the superstructure in $Pb_3M(PO_4)_3$. The formation of the $Sr_9V(PO_4)_7$ compound confirms indirectly this suggestion. One may expect a similar superstructure and ordering type in the Ti-containing eulytite-like compound $Pb_{3.5}Ti(PO_4)_3$ [12,27]. However, in this case an additional electron microscopy study is needed.

Acknowledgments

Authors are grateful to RFBR (Grant 04-03-32787) and ICDD (Grant-in-Aid APS91-05) for financial support. Part

of this work has been performed within the framework of the IAP 5-1 of the Belgian government.

References

[1] H. Liang, Y. Tao, Q. Su, Mater. Sci. Eng. B 119 (2005) 152–158.
[2] H. Liang, Y. Tao, J. Xu, H. He, H. Wu, W. Chen, S. Wang, Q. Su, J. Solid State Chem. 177 (2004) 901–908.
[3] B. Briat, A. Watterich, F. Ramaz, L. Kovács, B.C. Forget, N. Romanov, Opt. Mater. 20 (2002) 253–262.
[4] H.F. Folkerts, J. Zuidema, G. Blasse, Chem. Phys. Lett. 249 (1996) 59–63.
[5] T. Znamierowska, W. Szuszkiewicz, J. Hanuza, L. Macalik, D. Hreniak, W. Stręk, J. Alloys Compd. 341 (2002) 371–375.
[6] J. Barbier, J.E. Greedan, T. Asaro, G.J. McCarthy, Eur. J. Solid State Inorg. Chem. 27 (1990) 855–867.
[7] J. Barbier, J. Solid State Chem. 101 (1992) 249–256.
[8] E.H. Arbib, B. Elouadi, J.-P. Chaminade, J. Darriet, Mater. Res. Bull. 35 (2000) 761–773.
[9] Von G. Engel, W. Kirchberger, Z. Anorg. Allg. Chem 417 (1975) 81–88.
[10] E.H. Arbib, J.-P. Chaminade, J. Darriet, B. Elouadi, Solid State Sci. 2 (2000) 243–247.
[11] J. Barbier, Eur. J. Solid State Inorg. Chem. 31 (1994) 163–171.
[12] Von G. Engel, Z. Anorg. Allg. Chem 443 (1978) 23–27.
[13] R.V. Shpanchenko et al., to be published.
[14] K.K. Palkina, V.Z. Saifuddinov, A.V. Lavrov, Dokl. Akad. Nauk SSSR 237 (1977) 1090–1093 (in Russian).
[15] ICDD PDF2 Card #47-830.
[16] ICDD PDF2 Card #45-536.
[17] A.C. Larson, R.B. Von Dreele, Los Alamos National Laboratory Report LAUR 86–748 (1994).
[18] L.G. Akselrud, P.Yu. Zavalii, Yu.N. Grin, V.K. Pecharski, B. Baumgartner, E. Wölfel, Mater. Sci. Forum 133–136 (1993) 335.
[19] R.V. Shpanchenko, O.A. Lapshina, E.V. Antipov, J. Hadermann, E.E. Kaul, C. Geibel, Mater. Res. Bull. 40/9 (2005) 1569–1576.
[20] S. Boudin, A. Grandin, A. Leclaire, M.M. Borel, B. Raveau, J. Mater. Chem. 4 (1994) 1889.
[21] J. Barbier, D. Maxin, J. Solid State Chem. 116 (1995) 179–184.
[22] K. Hartl, R. Braumgart, Z. Naturforsch. B 33 (1978) 954–955.
[23] A.A. Tsirlin, E.V. Dikarev, R.V. Shpanchenko, E.V. Antipov, Acta Cryst. C (2005).
[24] H.-C. Liu, C.-L. Kuo, J. Mater. Sci. Tech. 13 (1997) 145–148.
[25] S.F. Radaev, L.A. Muradyan, Yu.F. Kargin, V.A. Sarin, V.N. Kanepit, V.I. Simonov, Kristallografiya 35 (1990) 361–364 (in Russian).
[26] H.N. Ng, C. Calvo, Can. J. Phys. 53 (1975) 42–51.
[27] D. Fahmi, B. Piriou, M. Zouiri, M.-R. Lee, M. Quarton, Eur. J. Solid State Inorg. Chem. 26 (1989) 313–325.